Revealing Differences in Anatomical Remodelling of the Systemic Right Ventricle

Ernesto Zacur[1(✉)], James Wong[2], Reza Razavi[2], Tal Geva[3], Gerald Greil[2], and Pablo Lamata[1]

[1] Department of Biomedical Engineering, King's College London, London, UK
ernesto.zacur@kcl.ac.uk
[2] Department of Imaging Sciences, King's College London, London, UK
[3] Boston Children's Hospital, Harvard Medical School, Boston, MA, USA

Abstract. Cardiac remodelling, which refers to the change of the shape and size of the myocardium, is an adaptive response to developmental, disease and surgical processes. Traditional metrics of length, volume, aspect ratio or wall thickness are used in the clinic and in medical research, but have limited capabilities to describe complex structures such as the shape of cardiac ventricles. In this work we present an example of how computational analysis of cardiac anatomy can reveal more detailed description of developmental and remodelling patterns. The clinical problem is the analysis of the impact of two different surgical palliation techniques for hypoplastic left heart syndrome. Construction of a computational atlas and the statistical description of its variability are performed from the short axis stack of 128 subjects. Results unveil, for the first time in the literature, the differences in remodelling of the systemic right ventricle depending on the surgical palliation technique.

Keywords: Computational anatomy · Statistical shape analysis · Systemic right ventricle · Discriminative analysis

1 Introduction

Hypoplastic left heart syndrome (HLHS) is a congenital heart defect where a baby is born with the left ventricle severely underdeveloped. This condition requires a three-stage surgical palliation procedure that creates a circulation based on the two chambers of the right side of the heart that is compatible with life. The first stage (called Norwood procedure) is performed within the first weeks after birth. This stage aims to improve systemic perfusion by reconstructing the native aorta and arch, maintain pulmonary perfusion via insertion of a shunt and promote mixing of blood with an atrial septectomy. A subsequent stage of surgery (Stage II or Glenn procedure) is performed at ages 4 to 6 months, and seeks to form a superior cavo-pulmonary anastomosis in order to provide a more permanent supply of blood to the lungs. The final procedure (Stage III or Fontan procedure), performed at 2 to 4 years of age, involves a total cavo-pulmonary anastomosis in order to separate oxygenated and deoxygenated circulation.

One of the following two techniques can be used in the Norwood procedure (Stage I) as systemic-to-pulmonary artery shunt to supply blood to the lungs:

H. van Assen et al. (Eds.): FIMH 2015, LNCS 9126, pp. 99–107, 2015.
DOI: 10.1007/978-3-319-20309-6_12

- The modified Blalock-Taussig (MBT) shunt creates a connection between the innominate or subclavian artery and one of the branch pulmonary arteries. Some studies have associated the MBT shunt with haemodynamic instability and sudden unexpected death as continuous flow of blood into the low resistance pulmonary circulation during diastole may lead to under-perfusion of the coronary arteries.
- The right ventricle-to-pulmonary artery (RVPA) shunt (a.k.a. Sano shunt) involves the placement of a conduit between the pulmonary artery and the right ventricle. RVPA reduces the risk of under-perfusion as the circulation is primarily in systole. However, this technique results in a scar on the wall of the systemic ventricle and increases the risk of arrhythmias or aneurysmal dilatation of the outflow tract.

Recent evidence showed an association of the RVPA shunt with a higher transplantation free survival at a year of age, although no differences in measures of RV ejection fraction (EF) were found [5]. At 32 months of age, RV EF had deteriorated significantly in the RVPA shunt group and transplant free survival rates were indistinguishable between the both shunt strategies. At present, and despite these evidences, the direct impact of the ventriculotomy scar on the growth and motion of systemic RVs remains incompletely understood.

Cardiac magnetic resonance (CMR) provides detailed 3D descriptions of the RV [1], but applying traditional scalar measurements such as volumes, lengths, thickness or diameters may be insufficient to capture complex variations in the geometry of 3D shapes. However, tools from the Computational Anatomy discipline, in particular shape analysis from CMR images, allow the analysis, detection and location of small differences in ventricular geometries. These tools are now applied in the medical research field, revealing detailed anatomical patterns in diseases and several findings in relationships between anatomy and organ function [3, 10, 18].

In this study we examine differences in the anatomical remodelling of the systemic RV in patients with HLHS who have undergone MBT or RVPA shunt techniques. Patient anatomies were expressed as the geometrical shape of the RV, extracted from dynamic CMR images. All shapes of RVs are considered to share the same geometrical features, and the differences between these features can describe the population variability. We describe shape variability by means of spatial coordinates of homologous points among geometries. Statistical techniques of dimensionality reduction enable the identification of differences in the cardiac remodelling between the two shunt techniques.

2 Materials and Methods

2.1 Cohort and Image Acquisition

In order to investigate the anatomical cardiac remodelling regarding the surgical shunt technique, a cohort of 128 patients of HLHS were analysed. Patient population presents differences in the Norwood technique and in the stage of the procedure. Demographic information is presented in Table 1.

Datasets were acquired at 2 congenital cardiac centres; MBT from Evelina London Children's Hospital, UK (ethical approval 08/H0810/058), while RVPA patients' data

were provided by Boston Children's Hospital, USA (ethical approval IRB-P00012488). Datasets consist of balanced steady state free precession (bSSFP) cine imaging in short axis orientations acquired on a 1.5-T Philips Achieva MRI scanner according to recent guidelines [4]. Images were acquired with pixel size varying from 0.85 to 1.4 mm in the short axis plane and from 5 to 10 mm inter-slice separation. Typically, the myocardial occupies from 6 to 13 slices depending on patient's heart size and inter-slice gap. CMR scans were acquired after Stage I at age 70 to 160 days, after Stage II at 20 to 35 months of age, and after Stage III at 3 to 14 years of age. Babies were scanned under anaesthetic.

Table 1. Demographic data.

	MBT shunt	RVPA shunt
Stage I	30	20
Stage II	29	14
Stage III	32	3
Total	91	37
Age at Norwood	7.1 ± 6.7 days	5.3 ± 2.8 days

2.2 Image Segmentation and Mesh Personalization

The systemic RV was assumed to have an elliptical shape, similarly to a healthy left ventricle (LV), and therefore it includes the septal wall. RV myocardium of all short-axis cine stacks was manually contoured by an expert at end-diastole. Trabeculations were excluded from the segmentation.

Segmented myocardial anatomies were fitted to a template mesh formed by cubic Hermite bricks [17] using the methods described in [8, 9]. The mesh fitting algorithm uses all slices with anatomical information of the systemic RV. Truncation of the basal ventricular anatomy was made at the image acquisition set, when the expert operator decides the plane that captures the most basal slice of the ventricles. A limited flexibility is provided to the template by means of the allowed degrees of freedom of the template. This results in a regularized fitting of the manual segmentation, reducing segmentation errors from human operation or from its discretized nature. All 128 scans were personalized reaching an average distance no larger than 1.5 mm to the manual segmentation. After the fitting step, the surfaces of the Hermite elements were tessellated into a triangular mesh. As a result of this process, the systemic RV anatomy was described by a set of 2834 descriptive points and each of these points is assumed to be in anatomical correspondence among all anatomies.

Differences in postural information were removed by pre-aligning all cases: all geometries were rotated to set the apical-base direction in the vertical Z axis and the right to left direction (identified by the centre of the LV blood pool manually located) in the horizontal X axis. Translational offset was removed by aligning the centre of RV blood pool. Finally, size is normalized by uniform scaling such that all segmented myocardia have a volume equal to the geometric mean of the original volumes. Notice that we are including geometries of hearts of ages from 3 months to 14 years old and

without the volume normalization the most important geometrical feature results to be the size. An alternative size normalization could be to consider clinical information such as subject's weight, height or age as was done in [11]. Nevertheless, in a preliminary study, we found that size is not a relevant remodelling pattern in this population. This also explains why traditional shape indexes (volume, mass) have not been able to identify differences between surgery procedures.

Even if CMR scans are from the same patient at different stages, the analyses performed in this work considered all the data independent as in a transversal study.

2.3 Statistical Description of the Data

A mean geometry was constructed from the 128 geometrical descriptors by averaging along the population the spatial coordinates of each descriptive point. This mean geometry (also called *anatomical atlas*) comprises the geometrical characteristics shared among all patients, see Fig. 1.

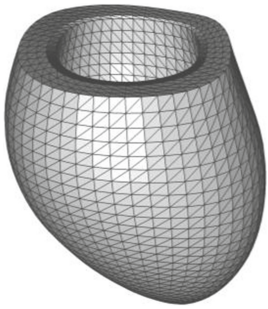

Fig. 1. Anatomical atlas (average shape of 128 cases) of the systemic right ventricle in HLHS. Shape coordinates characterise the differences in anatomy with respect to this mean shape.

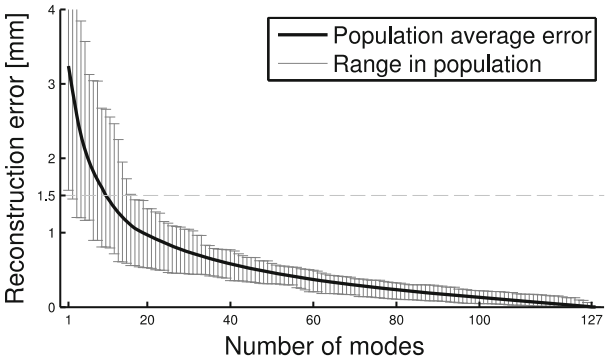

Fig. 2. Reconstruction error in terms of the number of PCA components. 16 PCA components are enough to reconstruct all instances within 1.5 mm of accuracy.

The residual geometrical information between the patients and the atlas is statistically analysed by means of principal components analysis (PCA) technique [6]. PCA

performs an orthogonal linear transformation formed by the sequence of the *most expressive features* [14]. It is important to note that in the PCA space, the more coordinates are considered to reconstruct the data, the more accurate the reconstruction is. Figure 2 shows reconstruction errors among 128 descriptors and among the 2834 descriptive points. It can be noted that 127 PCA coordinates are required to represent the whole population (instead of the 2834 × 3 coordinates required in the Cartesian description). By considering only 16 PCA coordinates, all reconstructed instances are within 1.5 mm of accuracy (same as the mesh personalization process described before). The truncation of PCA coordinates can be also considered as a filtering of low-SNR additive noise in the data [12]. Figure 3 illustrates these concepts through a gradual reconstruction of a contour with increasing number of PCA components.

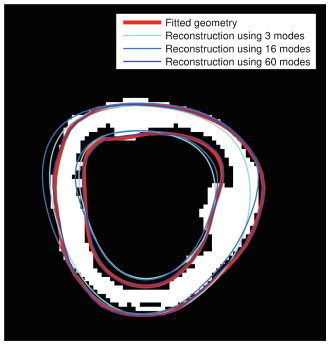

Fig. 3. Illustration of the mesh fitting and PCA reconstruction accuracy. It compares a segmented scan, subject to user and discretization/quantization/pixilation errors; the fitted geometry, stated to the regularization given in the fitting process; and corresponding reconstructed instances by taking into account different number of PCA components.

3 Qualitative Inspection and Quantitative Analysis

The principal modes in shape variation of the HLHS cohort, obtained by PCA, are illustrated in Fig. 4.

In order to perform a quantitative analysis of the discriminative properties of each mode, we performed a 'two-sample Student's *t*-test' [16] along each principal component. The Student's *t*-test has an associated *p*-value. This *p*-value indicates the degree of confidence that the instances of both groups correspond to random draws from two populations with different means. Without making strong assumptions on the underlying distribution of the data, the *p*-value can be empirically assessed with a randomized permutation test [7]. In a binary group discrimination task, the smaller the resulting *p*-value, the more distinguishable the groups are.

Specifically, we compute *p*-values between MBT *vs.* RVPA patient groups along the first 20 PCA coordinates. For each direction, the resulting *p*-value was computed by means of permutation test performed with 10^5 random permutations of the group label. The obtained *p*-value was used as an indication of the separability of the groups.

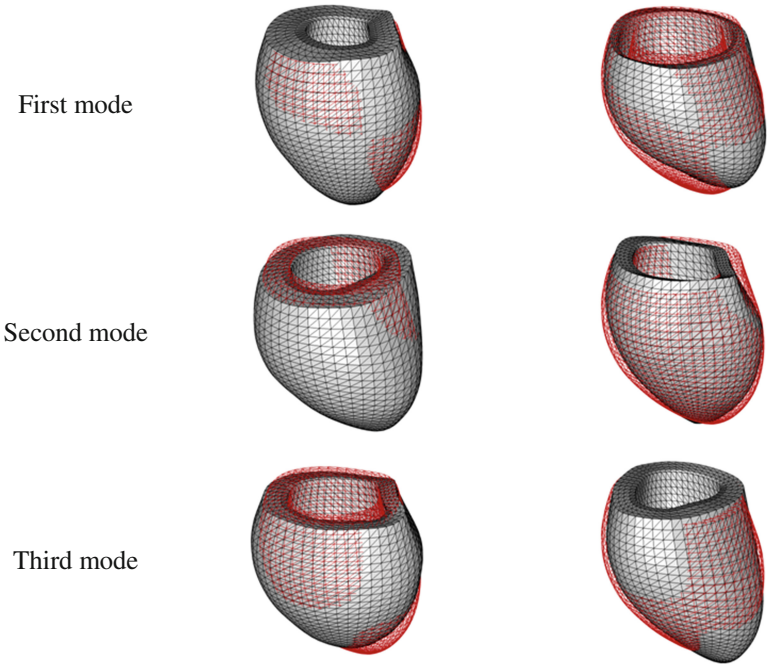

Fig. 4. Extremal shapes (*atlas* ± 2 std dev) along the first, second and third principal components directions. The atlas is shown in red to compare.

Figure 5 shows the *p*-values corresponding to *t*-test between subgroups MBT-Stage I *vs.* RVPA-Stage I and between subgroups MBT-Stage II *vs.* RVPA-Stage II. These results illustrate that groups are more similar between them at Stage I than at Stages II.

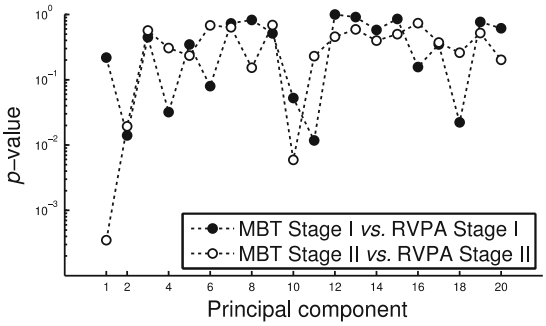

Fig. 5. *p*-values of the Student's *t*-test along each principal component. A significant difference at Stage II in mode 1 ($p < 0.001$) is revealed, without any other mode showing this level of significance at any of the two stages.

4 Revealing Anatomical Differences Between Surgical Techniques

It is expected that the impact of cardiac remodelling after the Norwood procedure increases along time, which is supported by results in Fig. 5. In order to illustrate the location of the most prominent remodelling differences between surgical techniques, a multivariate Hotelling's T2 test was performed for each descriptive point including its x,y,z coordinates [13]. Non-parametric permutation tests (with 10^4 random permutations) estimate the *p*-value of the T2 statistics. Subsequently, *false discovery rate* (FDR) correction [2] were used as control approach on simultaneous multiple comparisons. Figure 6 shows the corrected *p*-values obtained in the comparison between all-Stage I *vs.* MBT or RVPA at Stage II. This figure shows that the number of points with significant differences is much larger when Norwood procedure is performed by the RVPA than by the MBP shunt.

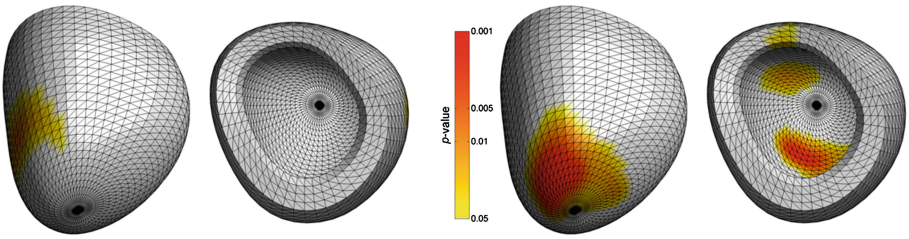

a) all-Stage I *vs.* MBT-Stage II b) all-Stage I *vs.* RVPA-Stage II

Fig. 6. Anatomical location of remodelling differences (FDR corrected *p*-value of Hotelling's T2 test for each descriptive point): BMT sub-group shows an almost empty map of differences, suggesting a simple growth from Stage I to Stage II, but RVPA subgroup shows a large region with statistically significant changes, indicating a different remodelling pattern.

5 Discussion and Conclusions

The computational analysis of the systemic RV anatomy has revealed remodelling differences between the two shunt surgical techniques. This finding has never been reported using traditional geometrical indexes, and illustrates the added value of the proposed methodology.

RVPA shunt is considered a *more aggressive* surgical technique than MBP shunt. The necessary ventriculotomy affects directly to the myocardium muscle and larger cardiac remodelling effects are expected. Our results are in agreement with this consideration: the differences at Stage II between the RVPA and MBP subgroups are mainly originated by a different remodelling pattern of RVPA subgroup compared to a simple growth of MBP subjects, see Fig. 6.

Besides known findings obtained from correlations between traditional scalar measurements, such as volumes, lengths, thickness or diameters, [1] the use of high dimensional shape descriptions may improve our understanding of the cardiac

remodelling. However, the use of such novel shape descriptions poses important challenges for its interpretation: a shape coefficient is a much more abstract and intangible number compared to traditional scalar measurements. We have dealt with this limitation by the illustration of the anatomical regions where changes are more significant, helping thus to extract valuable clinical conclusions from the data.

There are several limitations in this study. The construction of the computational atlas is limited to the available image resolution (a short axis stack). Full 3D resolution images would have revealed a higher level of anatomical detail. The automatic 3D mesh reconstruction of the systemic RV achieved a lower, although tolerable, accuracy compared to the adult healthy LV (average fitting error divided by average length: 1.43 mm/78 mm versus 1.28 mm/95 mm [10]), indicating the greater difficulty for manual segmentation and automatic reconstruction of a structure with thinner walls and larger shape variability.

HLHS is a condition with a very limited number of cases in the world (with a prevalence rate of two to three cases per 10,000 live births), and reaching statistical power from small study cohorts requires accurate biomarkers. Our results demonstrate the capability to quantify ventricular remodelling, which is a signature of the extra burden imposed to the systemic right ventricle. Moreover, in a recent parallel study we have identified the relationship between shape and function, where an RVPA shunt is also associated with an impaired contraction [15]. Shape metrics may thus help in understanding of the cardiac remodelling after the Norwood procedure. From a clinical viewpoint, shape metrics could improve the stratification and the planning of surgical procedures in subjects with HLHS, enable an early detection of maladaptive remodelling patterns, and guide the decisions for an optimal treatment.

Acknowledgements. This study has received funding by the Department of Health through the NIHR comprehensive Biomedical Research Centre award to Guy's & St Thomas' NHS Foundation Trust in partnership with King's College London and King's College Hospital NHS Foundation Trust, the Centre of Excellence in Medical Engineering (funded by the Wellcome Trust and EPSRC; grant number WT 088641/Z/09/Z) as well as the BHF Centre of Excellence (British Heart Foundation award RE/08/03). PL holds a Sir Henry Dale Fellowship funded jointly by the Wellcome Trust and the Royal Society (grant no. 099973/Z/12/Z).

References

1. Bellsham-Revell, H.R., Tibby, S.M., Bell, A.J., Witter, T., Simpson, J., Beerbaum, P., Anderson, D., Austin, C.B., Greil, G.F., Razavi, R.: Serial magnetic resonance imaging in hypoplastic left Heart syndrome gives valuable insight into ventricular and vascular adaptation. J. Am. Coll. Cardiol. **61**(5), 561–570 (2013)
2. Benjamini, Y., Hochberg, Y.: Controlling the false discovery rate: a practical and powerful approach to multiple testing. J. Roy. Stat. Soc.: Ser. B (Methodol.) **57**, 289–300 (1995)
3. Fonseca, C.G., Backhaus, M., Bluemke, D.A., Britten, R.D., Do Chung, J., Cowan, B.R., et al.: The Cardiac Atlas Project—an imaging database for computational modeling and statistical atlases of the heart. Bioinformatics **27**(16), 2288–2295 (2011)

4. Fratz, S., Chung, T., Greil, G.F., Samyn, M.M., Taylor, A.M., Valsangiacomo Buechel, E.R., Yoo, S.-J., Powell, A.J.: Guidelines and protocols for cardiovascular magnetic resonance in Children and Adults with congenital heart disease: SCMR expert consensus group on congenital Heart disease. J. Cardiovasc. Magn. Reson. **15**(1), 51 (2013)
5. Frommelt, P.C., Gerstenberger, E., Cnota, J.F., Cohen, M.S., Gorentz, J., Hill, K.D., et al.: Impact of initial shunt type on cardiac size and function in children with single right ventricle anomalies before the Fontan procedure: the single ventricle reconstruction extension trial. J. Am. Coll. Cardiol. **64**(19), 2026–2035 (2014)
6. Fukunaga, K.: Introduction to Statistical Pattern Recognition. Academic Press, San Diego (2013)
7. Good, P.I.: Permutation Tests: A Practical Guide to Resampling Methods for Testing Hypotheses. Springer, New York (2000). Springer Series in Statistics
8. Lamata, P., Niederer, S., Nordsletten, D., Barber, D.C., Roy, I., Hose, D.R., Smith, N.: An accurate, fast and robust method to generate patient-specific cubic Hermite meshes. Med. Image Anal. **15**(6), 801–813 (2011)
9. Lamata, P., Sinclair, M., Kerfoot, E., Lee, A., Crozier, A., Blazevic, B., et al.: An automatic service for the personalization of ventricular cardiac meshes. J. R. Soc. Interface **11**(91), 20131023 (2014)
10. Lewandowski, A.J., Augustine, D., Lamata, P., Davis, E.F., Lazdam, M., Francis, J., McCormick, K., et al.: Preterm Heart in adult life: cardiovascular magnetic resonance reveals distinct differences in left ventricular mass, geometry, and function. Circulation **127** (2), 197–206 (2013)
11. Medrano-Gracia, P., Cowan, B.R., Ambale-Venkatesh, B., Bluemke, D.A., Eng, J., et al.: Left ventricular shape variation in asymptomatic populations: the multi-ethnic study of atherosclerosis. J. Cardiovasc. Magn. Reson. **16**, 56 (2014)
12. Olmos, S., Garcia, J., Jané, R., Laguna, P.: ECG signal compression plus noise filtering with truncated orthogonal expansions. Sig. Process. **79**(1), 97–115 (1999)
13. Styner, M., Oguz, I., Xu, S., Pantazis, D., Gerig, G.: Statistical group differences in anatomical shape analysis using Hotelling T2 metric. In: Medical Imaging, International Society for Optics and Photonics, vol. 6512 (2007)
14. Swets, D., Weng, J.: Using discriminant Eigenfeatures for image retrieval. IEEE Trans. Pattern Anal. Mach. Intell. **18**, 831–836 (1996)
15. Wong, J., Lamata, P., Rathod, R.H., Bertaud, S., Dedieu, N., et al.: Using cardiac magnetic resonance and computational modelling to assess the systemic right ventricle following different Norwood procedures: a dual centre study. J. Cardiovasc. Magn. Reson. **17**(1), M12 (2015)
16. Woolson, R.F., Clarke, W.R.: Statistical Methods for the Analysis of Biomedical Data. Wiley, New Jersey (2011)
17. Young, A.A., Cowan, B.R., Thrupp, S.F., Hedley, W.J., Dell'Italia, L.J.: Left ventricular mass and volume: fast calculation with guide-point modeling on mr images. Radiology **216** (2), 597–602 (2000)
18. Zhang, X., Cowan, B.R., Bluemke, D.A., Finn, J.P., Fonseca, C.G., Kadish, A.H., et al.: Atlas-based quantification of cardiac remodeling due to myocardial infarction. PLoS ONE **9** (10), e110243 (2014)